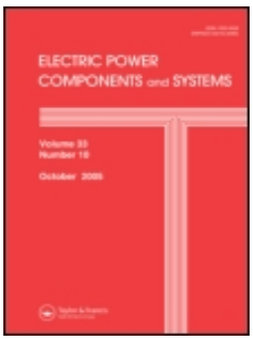

Taylor & Francis
Taylor & Francis Group

Electric Power Components and Systems

ISSN: 1532-5008 (Print) 1532-5016 (Online) Journal homepage: http://www.tandfonline.com/loi/uemp20

Position Sensorless Control of a Reluctance Synchronous Wind Generator Drive with an LC Inverter Filter

Wikus T. Villet & Maarten. J. Kamper

To cite this article: Wikus T. Villet & Maarten. J. Kamper (2015) Position Sensorless Control of a Reluctance Synchronous Wind Generator Drive with an LC Inverter Filter, Electric Power Components and Systems, 43:8-10, 1051-1061, DOI: 10.1080/15325008.2015.1023909

To link to this article: http://dx.doi.org/10.1080/15325008.2015.1023909

Electric Power Components and Systems, 43(8–10):1051–1061, 2015

ISSN: 1532-5008 print / 1532-5016 online
DOI: 10.1080/15325008.2015.1023909

Taylor & Francis
Taylor & Francis Group

Position Sensorless Control of a Reluctance Synchronous Wind Generator Drive with an LC Inverter Filter

Wikus T. Villet and Maarten. J. Kamper
Department of Electric and Electronic Engineering, Stellenbosch University, Stellenbosch, South Africa

CONTENTS

Abstract—A control structure for an inverter-fed high speed reluctance synchronous generator wind energy conversion system is proposed and investigated in this article. The novel combination of an LC inverter output filter and a hybrid position sensorless control method is used to ensure robustness and reliability of the system. The proposed LC inverter filter and position sensorless control method also allows the inverter unit to be stationed in the tower base instead of in the nacelle. With the LC filter, sinusoidal machine terminal voltages and reduced electromagnetic interference (EMI) from the tower supple cables are ensured. A new estimation method is developed to minimize current and voltages sensors in the drive system with the LC filter, whereby the machine's stator quantities are estimated, requiring only parameter knowledge of the LC filter. The proposed hybrid position sensorless control algorithm uses the estimated stator quantities to estimate the rotor position. A high-frequency injection position sensorless control method is used at low speeds. The frequency of the high-frequency injection voltage is chosen close to the resonance frequency of the filter and machine model to amplify the high-frequency current response. Excellent dynamic performance of the proposed control drive system is obtained from a 9.6-kW laboratory reluctance synchronous generator drive system.

Keywords: control, position sensorless, reluctance synchronous, wind generator, inverter, LC filter

Received 28 November 2014; accepted 15 January 2015

Address correspondence to Prof. Maarten. J. Kamper, Electric Machines Laboratory, Department of Electric and Electronic Engineering, Private Bag X1, 7602 Matieland, Stellenbosch University, Stellenbosch, 7600, South Africa. E-mail: E-mail: Kamper@sun.ac.Za.

Color versions of one or more of the figures in the article can be found online at www.tandfonline.com/uemp.

1. INTRODUCTION

Wind turbine generator systems are distinguished by fixed-speed and variable-speed systems. Fixed-speed systems are characterized by the no-use of power electronic converters with the generator connected directly to the grid. Recent development of such a system was explained in [1]. Variable-speed systems on the other hand are characterized by the use of partially rated or fully rated power electronic converters. Two variable-speed turbine concepts are favored by the industry. The first is the most widely used generator, the doubly fed induction generator (DFIG), with a multi-stage gearbox and a partially rated converter [2].

The second industry-favored variable-speed wind turbine configuration has a fully rated converter. Topologies vary from squirrel-cage induction generators (SCIGs), wound rotor synchronous generators, and permanent magnet synchronous

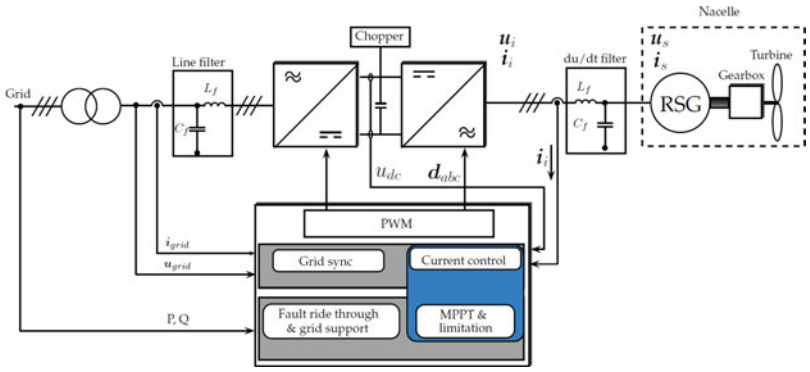

FIGURE 1. General control structure for a variable-speed wind turbine system.

generators (PMSGs) [3]. Also, drivetrains vary from multi-stage gearboxes, reduced stage gearboxes, and direct-drive topologies with high pole number permanent magnet (PM) generators. It was reported in [3] that the advantages of the full-scale converter setup over the partial converter DFIG setup are the possible elimination of slip rings, full speed and power controllability, better grid support, and better grid code compliance. It was suggested in [2] that variable-speed wind turbines with full-scale converters will dominate in large wind farm topologies in the future.

1.1. Control of Converter-fed Wind Turbines

The control structure for a general wind turbine system, as presented in [3–6], is shown in Figure 1. A current controller is used to control the generator torque and by that the rotor speed for maximum power generation [3]. The grid-side converter controls the active and reactive power to and from the grid [7]. Wind turbine specific control includes maximum power point tracking (MPPT), pitch control, low-voltage ride through, and providing grid support [3].

It is still not clear whether direct torque control (DTC) or field-oriented control (FOC) is best suited for control of wind turbines. Some large wind turbine manufactures have completely adopted DTC in their position sensorless wind turbine converters [8]. FOC exhibits good torque response, accurate speed control, and achieves full torque at zero speed [9]. FOC, however, needs to be extended to be position sensorless so as to avoid using fragile position sensors. The advantages of DTC is its dynamic behavior and that it is inherently position sensorless. The main disadvantages of DTC are the variable switching frequency, high torque pulsations, and fast sampling time requirements [9]. The DTC method can be extended with space vector modulation (SVM). The DTC-SVM method has the advantage of a constant switching frequency and reduced torque ripple compared to DTC [10]. The electrical rotor position is also a requirement for DTC-SVM methods, however, and thus also needs to be extended to be position sensorless [11].

1.2. Inverter Output Low-pass Filter

In [12, 13], it was stated that the rectangular waveform created by pulse width modulation (PWM) inverters can cause several problems on the machine cables and at the machine terminals. It is therefore suggested that an LC filter be inserted between the inverter and the machine to ensure sinusoidal machine voltages and to reduce the over-voltage peaks caused by the fast voltage rise time and switching frequency. This filter is referred to as a du/dt filter and is used in various industry converters [5, 6, 14].

LC filters on long cables also prevent voltage reflections that may cause voltages spikes of twice the DC bus voltage at the motor terminals, damaging the machine insulation [12, 13, 15, 16]. The rate of voltage rise can also cause bearing currents in the machine and electromagnetic interference (EMI), which can be prevented with an inverter output LC filter [13, 16].

1.3. The Inverter-fed Reluctance Synchronous Generator (RSG)

Not much literature exists on the subject of inverter-fed RSGs. A voltage source inverter-fed RSG was proposed in [17, 18]. The proposed super-high-speed reluctance generator application is aimed at aircraft carriers, space shuttles, and deep sea marine applications. The implementation in [17, 18] requires the information from an encoder and has no inverter output LC filter. An axial laminated RSG was proposed in [19], where it was shown that the iron losses in the machine contribute to the power factor of the reluctance motor but reduce the power factor of the reluctance generator [19]. In [19], it was shown that for high efficiency and power factor, the inductance ratio L_d/L_q of the RSG needs to be high.

1.4. Position Sensorless Controlled Variable-speed Generators

The axial laminated RSG presented in [19] was controlled position sensorless with a model-based DTC implementation in [20]. The method proposed in [20] was only able to control the generator in the medium-to high-speed region. Simulation and measured results are thus all at high speed. No LC filter is used with this implementation. An inverter output LC filter can cause many well-known position sensorless control methods to fail at standstill according to [21]. A saliency based PWM injection method, which is able to estimate the electrical angle of a PM synchronous machine (PMSM), with an inverter output filter at standstill is proposed in [21]. The drawback of this method is the need to measure the stator current on the machine side of the LC filter. The stator and inverter current can differ due to the effect of the filter; thus, the inverter current needs to be measured as well to prevent damage to the drive. A similar method was presented in [22] for an undersea propulsion system.

A high-frequency (HF) injection position sensorless control method is used in [23] to control a PMSM with an inverter output LC filter. In this implementation the only measured quantities are the inverter phase current and the DC bus voltage. A mathematical model of the machine and the filter is used to estimate the stator quantities by deriving linear machine equations in [23].

2. PROPOSED RSG SETUP

It was pointed out in [24] that a wind turbine system with a lower efficiency that delivers energy at a lower cost is a better solution than a high-efficiency, high-cost system. It is thus important to minimize the cost of energy delivered [24]. A converter-fed RSG is proposed as an alternative to conventional variable-speed concepts. The RSG is cheaper to manufacture than SCIGs, DFIGs, wound rotor synchronous generators, and PMSGs. Not only is manufacturing of the RSG cheap, but research has also shown that the efficiency of the reluctance synchronous machine (RSM) compares well to that of the induction machine (IM), if not better [25, 26].

The RSG is brushless and is able to perform variable-speed operation through the entire speed range unlike the DFIG, which makes use of brushes. The RSG is a high-speed machine and would thus use a similar multi-stage gearbox as the SCIG and the DFIG. The high-efficiency and single-stage, or no gearbox, setup of the PMSG seems more attractive than the multi-stage gearbox RSG setup. The disadvantage of the PMSG turbine setup, however, is the large quantities of expensive PM material that is used and the increased nacelle mass. Manufacturing complexity is also high for large-power PMSGs. The RSG can thus be seen as an attractive alternative to the conventional fixed-speed and variable-speed wind turbine setups.

The aim of this research is to propose and implement an RSG wind energy conversion (WEC) system that is robust, reliable, and requires minimum maintenance. It is well known that the RSG is robust and reliable. The proposed turbine setup will thus not make sense if some other part of the WEC system is unreliable. It was reported in [27] that $\pm 14\%$ of turbine failures per year is as a result of frequency converter failure contributing to 18% of the yearly turbine downtime. Converter failure results in the second longest turbine downtime accumulated hours per year after pitch control failure [27].

Recently some companies have started installing the converter in the tower base instead of the nacelle [6, 28]. Some of the benefits listed in [28] are "reduced nacelle weight and size, vibrations sensitive components are stationary, more efficient maintenance and easier to replace components if necessary." The power converter location of the AREVA M5000-116 wind turbines, situated in the Alpha Ventus offshore wind farm off the coast of Germany, are also located in the tower base [29].

The proposed RSG setup is as shown in Figure 1. This implementation allows all the power electronics and controllers to be stationed in the tower base. Although this will not necessarily improve the reliability of the converter, this might reduce the downtime of the turbine during maintenance of the converter. The weight of the nacelle is thus also reduced. It must further be noted that the power converter can also be at medium voltage [6]. For the tower-based converter, an LC filter is necessary due to the long cables between the converter and generator. The LC inverter output filter will ensure sinusoidal machine voltages to reduce insulation deterioration, bearing currents, and EMI. The LC filter also allows unshielded cables to be used.

The only measurable quantities in the proposed setup are the DC bus voltage and the inverter currents. No additional measuring probes are necessary, thus reducing the risk of device failure. The most important feature of this setup is the omission of the position sensor. Complex electronic circuitry are required to use high-resolution position sensors over large lengths. The complexity and reliability of the WEC system is thus improved. Only the generator side of the converter, which is highlighted in Figure 1, is considered in this article. Subscript i in Figure 1 identifies inverter quantities, i.e., the voltage or current on the inverter side of the filter. Subscript s identifies the stator quantities; symbol $\boldsymbol{d}_{abc}$ represents the inverter switching states.

3. INVERTER OUTPUT LC FILTER AND STATOR QUANTITIES ESTIMATIONS

The addition of the LC filter not only affects the classic control structure of the RSG but also the position sensorless control methods, as will be explained in this section. The cut-off frequency of the LC inverter output filter needs to be designed to be well below the switching frequency of the drive but higher than the fundamental frequency of the machine. The transfer function of the LC filter is as shown in Eq. (1). In Eq. (1), L_f, C_f, and R_f are the filter inductance, capacitance and series resistance respectively. The cut-off frequency can be calculated by Eq. (2) [30]:

$$H_d(s) = H_q(s) = \frac{\frac{1}{L_f C_f}}{s^2 + s\frac{R_f}{L_f} + \frac{1}{L_f C_f}}, \tag{1}$$

$$f_o = \frac{\omega_o}{2\pi} = \frac{1}{2\pi\sqrt{L_f C_f}}. \tag{2}$$

By decoupling the speed voltage terms in the machine voltage equations, the machine transfer function can be derived as an inductive and resistive load, as shown by Eqs. (3) and (4):

$$\frac{i_d(s)}{u_d(s)} = \frac{1}{L_d s + R_s}, \tag{3}$$

$$\frac{i_q(s)}{u_q(s)} = \frac{1}{L_q s + R_s}. \tag{4}$$

The machine and filter parameters are summarized in Table 1. To evaluate the effect of the LC filter on the frequency response of the plant, it is necessary to evaluate the combination of the LC filter and plant transfer function. The bode plot of the d- and q-axis transfer functions at rated conditions is displayed in Figures. 2(a) and 2(b). The combination of the

Machine parameters	
Stator resistance R_s	0.15 Ω
Direct-axis inductance L_d	23.8 mH
Quadrature-axis inductance L_q	4.41 mH
Pole pairs N_p	2
Rated speed	1500 rev/min
Rated current (RMS)	40 A
Rated torque	61 Nm
Rated power	9.6 kW
Constant current angle ϕ	67°
Drive parameters	
Switching frequency F_s	6.1 kHz
Sampling frequency f_s	12.2 kHz
DC bus voltage u_{dc}	540 V
LC filter parameters	
Inductance L_f	1.33 mH
Capacitance C_f	25 μF
Series resistance R_f	0.2 Ω
Cut-off frequency f_o	872.82 Hz

TABLE 1. Machine and LC filter parameters

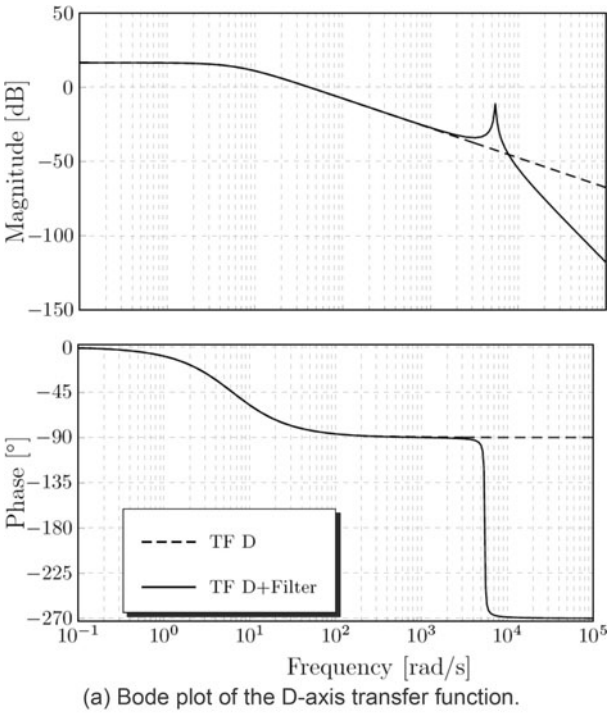

(a) Bode plot of the D-axis transfer function.

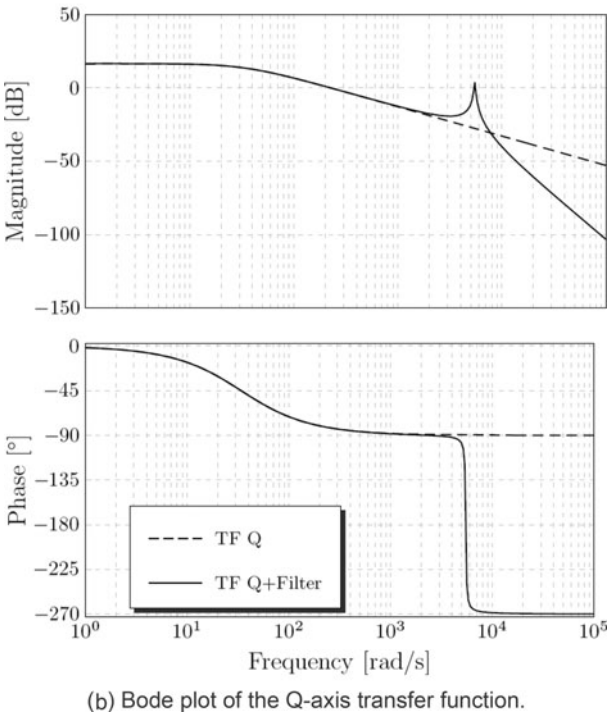

(b) Bode plot of the Q-axis transfer function.

FIGURE 2. Bode plots of the RSG with and without the inverter output filter.

plant transfer functions and LC filter are also plotted in Figures. 2(a) and 2(b). These graphs clearly show that the filter adds a resonance frequency to the plant and cuts-off after f_o. The importance of this resonance frequency with respect to the position sensorless control of the generator is explained later.

It is shown in Figure 1 that the only measurable quantities in the proposed WEC system are the DC bus voltage and the inverter current. The inverter and stator currents, however, are not the same due to the current flow in the capacitor. The inverter or reference control voltages are also not equal to the stator voltage during transients. The effect of the difference in inverter and stator quantities on the RSG control structure can be summarized as:

- $\boldsymbol{i}_i^s = \boldsymbol{i}_s^{s*} \neq \boldsymbol{i}_s^s$: The reference current in the control structure and the stator current are not equal, therefore affecting the MPPT of the generator.
- $\boldsymbol{i}_i^s \neq \boldsymbol{i}_s^s$ & $\boldsymbol{u}_s^{s*} \neq \boldsymbol{u}_s^s$: Flux linkage estimations that are used with the fundamental saliency position sensorless control method will be inaccurate and can thus cause this method to fail.

Adding stator current and - voltage measurement sensors is possible, but it is preferable not to add any additional measuring sensors to the WEC system. In [23, 31], the authors used a linear mathematical derivation of the machine as well as the LC filter model to calculate the stator voltages and currents. The machine used in [23, 31], however, have nearly constant d- and q-axis inductances. The d- and q-axis inductance of the RSG is non-linear as a function of current, and lookup tables will be necessary to estimate the stator quantities of the RSM. It is thus proposed to use only the mathematical model of the filter to estimate the stator currents and voltages. The combined RSG and LC filter voltage equation in vector format in the $\alpha\beta$ reference frame is as in Eq. (5):

$$\boldsymbol{u}_i^s = L_f \frac{d\boldsymbol{i}_i^s}{dt} + \boldsymbol{u}_s^s + R_f \boldsymbol{i}_i^s. \tag{5}$$

The machine's stator voltage is equal to the filter capacitor voltage, i.e.,

$$\boldsymbol{u}_s^s = \frac{1}{C_f} \int \boldsymbol{i}_c \, dt. \tag{6}$$

Now substitute Eq. (6) into Eq. (5) and rewrite into its Laplace equivalent equation:

$$\boldsymbol{u}_i^s(s) = sL_f \boldsymbol{i}_i^s(s) + \frac{1}{sC_f} \boldsymbol{i}_c(s) + R_f \boldsymbol{i}_i^s(s). \tag{7}$$

It is assumed that the rate of change of the current in the machine is much slower than that of the capacitor during transients. This assumption validates Eq. (8) and allows Eq. (7) to be derived as a function of stator voltage as in Eq. (9):

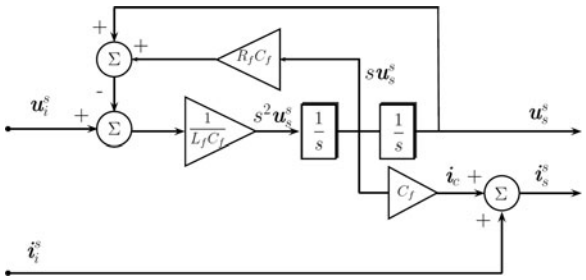

FIGURE 3. Schematic of stator quantity estimation method.

$$\boldsymbol{i}_i^s(s) = \boldsymbol{i}_c(s) = sC_f \boldsymbol{u}_s^s(s), \tag{8}$$

$$\begin{aligned} \boldsymbol{u}_i^s(s) &= s^2 L_f C_f \boldsymbol{u}_s^s(s) + \frac{1}{sC_f} sC_f \boldsymbol{u}_s^s(s) + sR_f C_f \boldsymbol{u}_s^s(s) \\ &= (s^2 L_f C_f + sR_f C_f + 1)\, \boldsymbol{u}_s^s(s). \end{aligned} \tag{9}$$

Reshuffling yields

$$\boldsymbol{u}_s^s(s) = \Big(\frac{\boldsymbol{u}_i^s(s) - sR_f C_f \boldsymbol{u}_s^s(s) - \boldsymbol{u}_s^s(s)}{s^2 L_f C_f} \Big). \tag{10}$$

Equations (10) and (6) can be used to estimate the stator voltage and the capacitor current. The capacitor current can be used to calculate the actual machine current. This estimation scheme is displayed in Figure 3.

4. POSITION SENSORLESS CONTROL IMPLEMENTATION

The position sensorless control method used is a hybrid method as presented in [32]. This method utilizes an alternating HF injection method at low speeds to standstill and a fundamental saliency position sensorless control method at a minimum to high speeds. The stator quantities that are estimated with the method displayed in Figure 3 are used for position estimation. The estimated stator current is also used as feedback for the current controller instead of the inverter current. The working of this setup is shown in Figure 4, Where PSC refers to position sensorless control. Transformation between reference frames are done with transformation matrices $\boldsymbol{T}$ and $\boldsymbol{T}^{-1}$. Estimated quantities are indicated with a hat.

The machine and filter transfer function frequency response in Figure 2 show that there is a peak resonance frequency created by the filter. This peak needs to be above the fundamental frequency but low enough to ensure sinusoidal phase voltages. This resonance peak can be used to design the control parameters for the HF injection position sensorless control method. The injected voltage will be amplified if its frequency

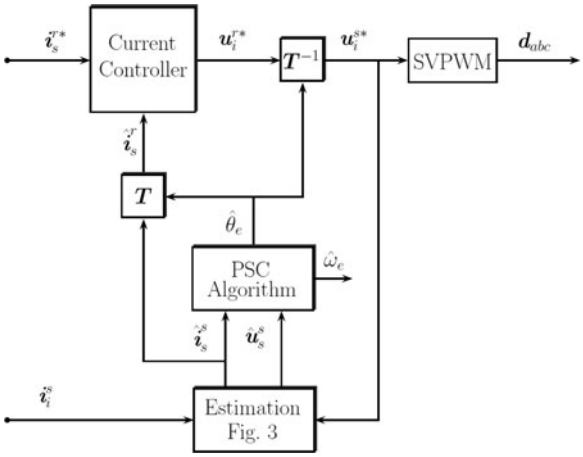

FIGURE 4. Position sensorless controller.

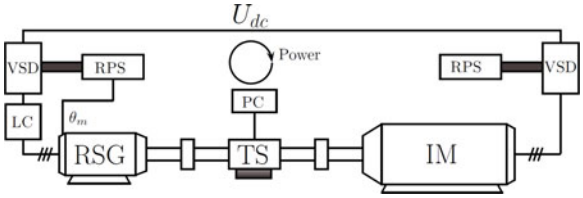

FIGURE 5. Diagram of laboratory setup used to test the RSG drive system.

is chosen in the vicinity of the resonance frequency allowing the injection voltage magnitude to be reduced. However, if the injection frequency is too close to the resonance frequency, the HF stator voltages and currents might be dangerously high [23].

As stated by [23], it is advisable to choose the injection frequency just below the resonance frequency to prevent dangerously high stator quantities but high enough to allow the filter to boost the HF current response. The filter thus aids the HF injection position sensorless control with this methodology instead of damping the HF response. The injection frequency for this system is chosen at 716 *Hz* by experimental implementation. The injection voltage is reduced from 66 to 33 *V* by using the LC filter to boost the HF current response.

The fundamental saliency position sensorless control method is used to control the generator in the medium-to high-speed regions as part of the hybrid position sensorless control methodology. This method makes use of lookup tables for position estimation. No literature currently exists of an implementation of this method with an inverter output filter. It is found during implementation that this method is unstable if the inverter quantities are used with the lookup table instead of the estimated stator quantities. The derived stator quantities estimation method thus stabilizes the fundamental saliency position sensorless control method. It is also found that the load-dependent compensation curve differs with and without the LC filter connected. It is thus essential that this curve be measured with the LC filter connected.

5. MEASURED RESULTS

A laboratory test bench is used to test and evaluate a 9.6 kW prototype RSG drive system, as shown in Figure 5. Two rapid prototyping systems (RPSs) are each connected to a variable speed drive (VSD). The one VSD has a 3-phase LC filter connected between its output terminals and the 9.6 kW RSG. The rotor position θ_m of the RSG is measured with a rotary encoder and fed back to the RPS. This measured position and speed, however, are not used in the control of the RSG but only to determine the quality of the position sensorless control method.

The RSG is connected via a torque sensor (TS) to a 45 kW IM that emulates the turbine and gearbox system. A personal computer (PC) is connected to the TS and is used to measure and record the shaft torque, power, and speed. The RPS allows the user to program and implement specific speed and/or torque steps via the IM to the RSG drive system. The DC buses of the two VSDs are connected allowing the power to circulate within the system.

5.1. Evaluation of the LC Filter and Stator Quantities Estimation Method

High-voltage differential probes are used to measure the line–line voltage on both sides of the LC filter to investigate its effectiveness at rated conditions. It is shown in Figure 6(a) that the inverter voltage u_{iab} is rectangular. The rectangular shape is caused by the switching of the semi-conductors. The machine terminal voltage u_{sab}, as shown in Figure 6(a) is sinusoidal as a result of the LC inverter output filter. The fast Fourier transform (FFT) of the inverter voltage u_{iab} is as shown in Figure 6(b). It is clear that the inverter voltage is very noisy. The FFT of the stator voltage, u_{sab} in Figure 6(c), shows that almost all of the switching harmonics are filtered out by the LC filter and only the fundamental 50 Hz harmonic remains. The x-axis of the results window is limited to 1.2 kHz to ensure that the fundamental harmonic is visible.

High-voltage differential probes are used in a second test to measure the a- phase voltages while generating rated power with the hybrid position sensorless control method. The measured inverter phase voltage u_{ia} is shown in Figure 7(a). The measured stator phase voltage u_{sa}, applied to the machine terminals, as well as the estimated phase voltage $\hat{u}_{sa}$, are also shown in Figure 7(a). These results show that the phase volt-

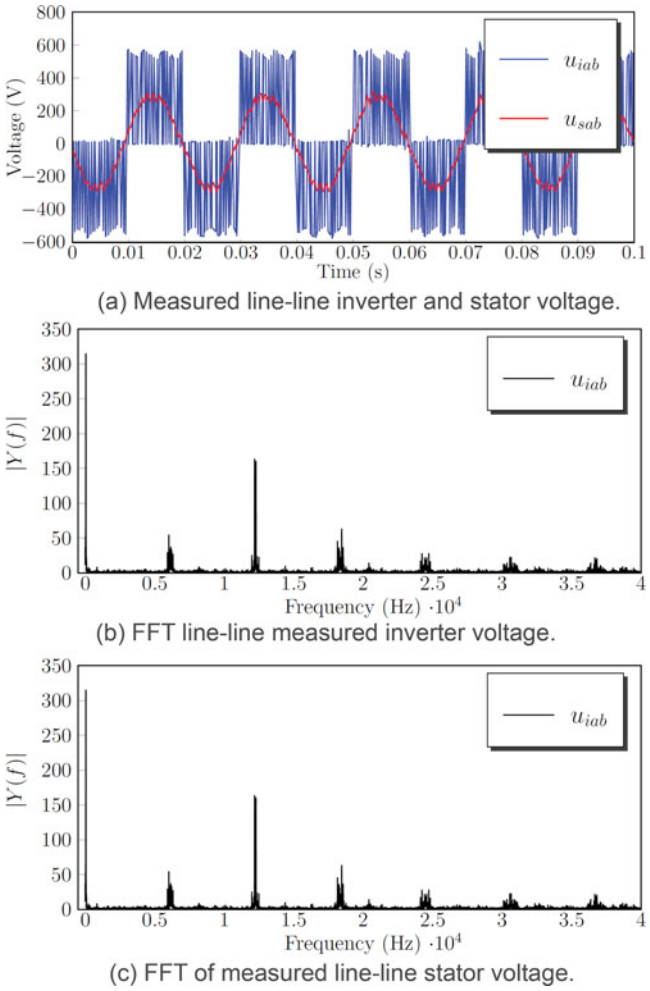

FIGURE 6. Measured line–line voltage on the inverter and machine side of the LC inverter output filter.

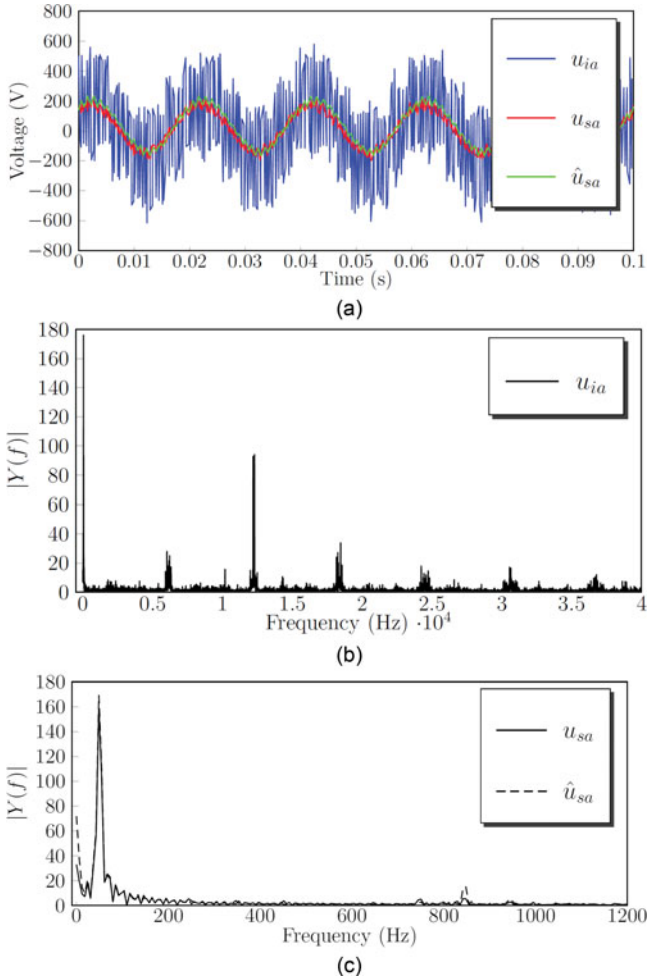

FIGURE 7. Measured and estimated phase voltage on the inverter and machine side of the LC inverter output filter: (a) measured and estimated phase inverter and stator voltages, (b) FFT of measured inverter phase voltage, and (c) FFT of measured and estimated stator phase voltages.

age applied to the machine is sinusoidal due to the LC low-pass filter. It is also shown in Figure 7(a) that the estimation scheme (Figure 3) is successful in estimating the stator phase voltage. There is a slight phase difference between the measured and estimated stator voltage, however. The FFT of the *a*- phase inverter voltage, as shown in Figure 7(b), shows that this voltage signal is very noisy. The FFT of the stator phase voltage and the estimated stator phase voltage correlate well, as shown in in Figure 7(c), where only one distinct fundamental harmonic is shown. Again, the results window is narrowed to display the fundamental harmonics.

Finally, a current measuring probe is used to measure the *a*- phase stator current i_{sa} while generating rated power. This measured current is shown in Figure 8(a) as well as the measured inverter current i_{ia} and the estimated stator current $\hat{i}_{sa}$. Figure 8(b) is a zoomed in window of Figure 8(a) and shows that the inverter and stator current differ during the negative peak of the sine wave. It is shown in Figure 8 that the stator quantity estimation scheme (Figure 3) is able to estimate the stator current during the negative peak of the sine wave within a satisfactory degree of accuracy.

The measured results of this section shows that sinusoidal voltages are supplied to the the terminals of the RSG via the LC filter. It is also shown that the performance of the derived voltage and current estimation method is satisfactory.

5.2. Torque Reference-based MPPT

The objective of MPPT is to adjust the speed of the turbine blades to operate on the maximum power point of the turbine as the wind speed varies [11]. The MPPT scheme implemented is torque reference-based MPPT. Equation (11)

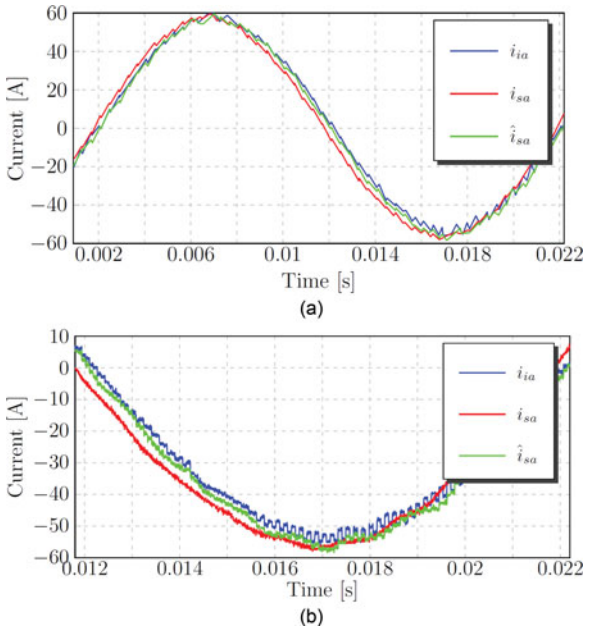

FIGURE 8. Measured and estimated phase current at full load: (a) measured and estimated phase current and (b) zoomed in measurement of Figure 8(a).

can be used in the control structure as the reference torque with the estimated mechanical speed of the generator [11]. K_{opt} is a turbine specific parameter. It is thus clear that the wind speed is not needed to implement torque reference-based MPPT:

$$T_m^* = K_{opt}\hat{\omega}_m^2. \tag{11}$$

The maximum torque curve equation can be calculated by determining K_{opt}. Alternatively, the maximum torque curve can be measured experimentally as a function of turbine speed [33]. This maximum torque curve can be represented by an equation or lookup tables. The optimal torque curves of wind turbines are usually proprietary information of the manufacturer. An optimal torque curve is thus created for this project for laboratory testing. Equation (12) is the assumed MPPT function used for laboratory testing. This function is derived to allow rated power generation at rated generator speed:

$$\mathbf{i}_s^{r*} = \frac{i_{rated}}{\omega_{rated}} * \hat{\omega}_m. \tag{12}$$

The reference current, as calculated from Eq. (12), is low-pass filtered with a digital low-pass filter in the control structure. This ensures that smooth torque is always applied by the generator even during wind spikes.

5.3. Evaluation of the Position Sensorless Controlled RSG

The next step is to verify the combined effectiveness of the MPPT, hybrid position sensorless control, and stator quantity estimation method. The generator speed and torque is measured and stored during testing with the torque and speed sensor device. The MPPT equation, Eq. (12), is used offline in MATLAB (The Mathworks, Natick, Massachusetts, USA) with the measured speed to calculate reference generator current, $\boldsymbol{i}_s^{r*}$. The calculated reference current is interpolated in MATLAB on a three-dimensional torque map of the machine to calculate the MPPT reference torque, $T_m(FE)$. This torque map is acquired from a finite-element package. The MPPT reference torque is compared to the measured generator torque. Figure 9 is a schematic representation of how this procedure is implemented.

The results of a speed ramp test are shown in Figure 10. In this test, the IM ramps its speed up from standstill to rated frequency. The measured speed sensor speed is shown in Figure 10(a), the measured TS torque ($T_m(T)$) and MPPT FE torque ($T_m(FE)$) in Figure 10(b), and finally the measured shaft power ($P_m(TS)$) and the MPPT FE calculated power ($P_m(FE)$) in Figure {\bf 10(c). It is clear that the torque and power of the position sensorless controlled RSG drive correlates well with the MPPT torque and power.

It is well known that the addition of an LC inverter output filter can damp the dynamic response of the inverter-fed electrical machine its position sensorless control performance. The dynamic behavior of the position sensorless controlled RSG with the inverter ouput filter is investigated by varying generator speed sinusoidally with the IM as shown in Figure 11(a). The MPPT reference torque should also vary sinusoidally as a function of speed according to Eq. (12). The machine response at different frequencies and amplitudes is investigated. The results of one of these tests are displayed in Figure 11. The results in Figure 11 show that the hybrid position sensorless control method is able to control the RSG dynamically, even though the conditions are more dynamic than what will be expected of a wind generator. It is shown in Figure 11(b) however, that there are instances where the measured torque ($T_m(T)$) does not correlate with the MPPT torque ($T_m(FE)$). This is

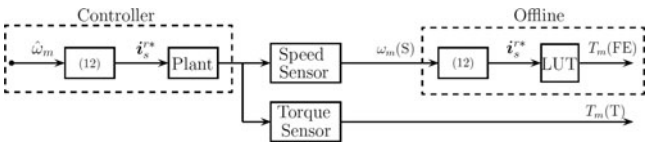

FIGURE 9. Method of comparing measured torque of the RSG with the MPPT reference torque obtained from FE.

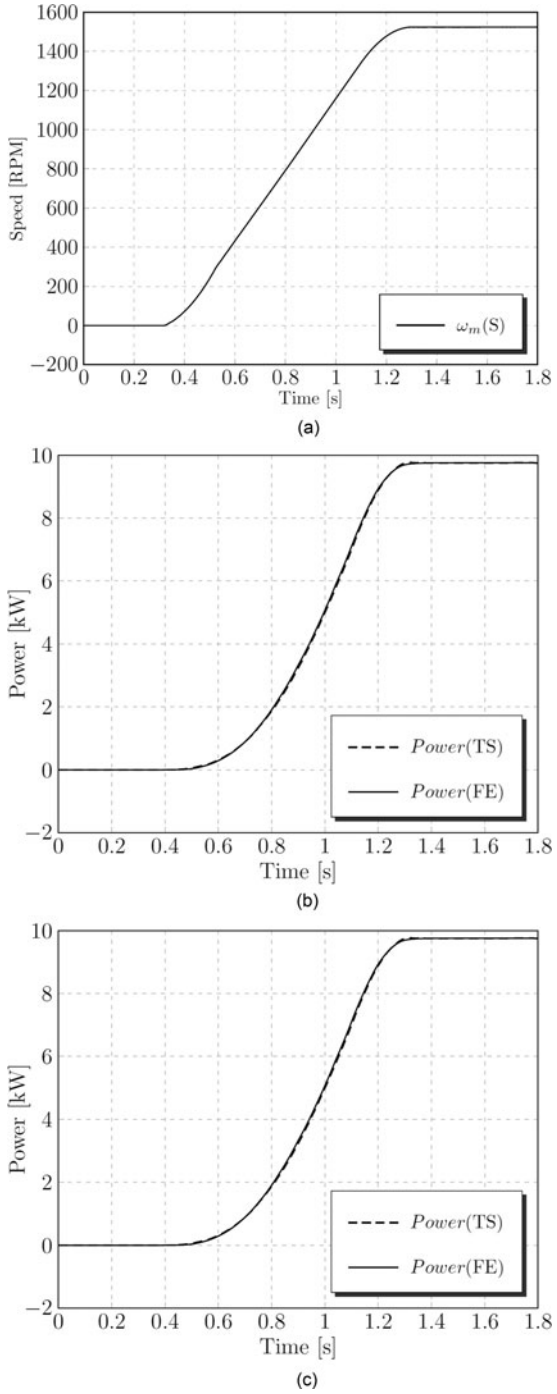

FIGURE 10. Measured speed ramp test of the position sensorless controlled RSG drive.

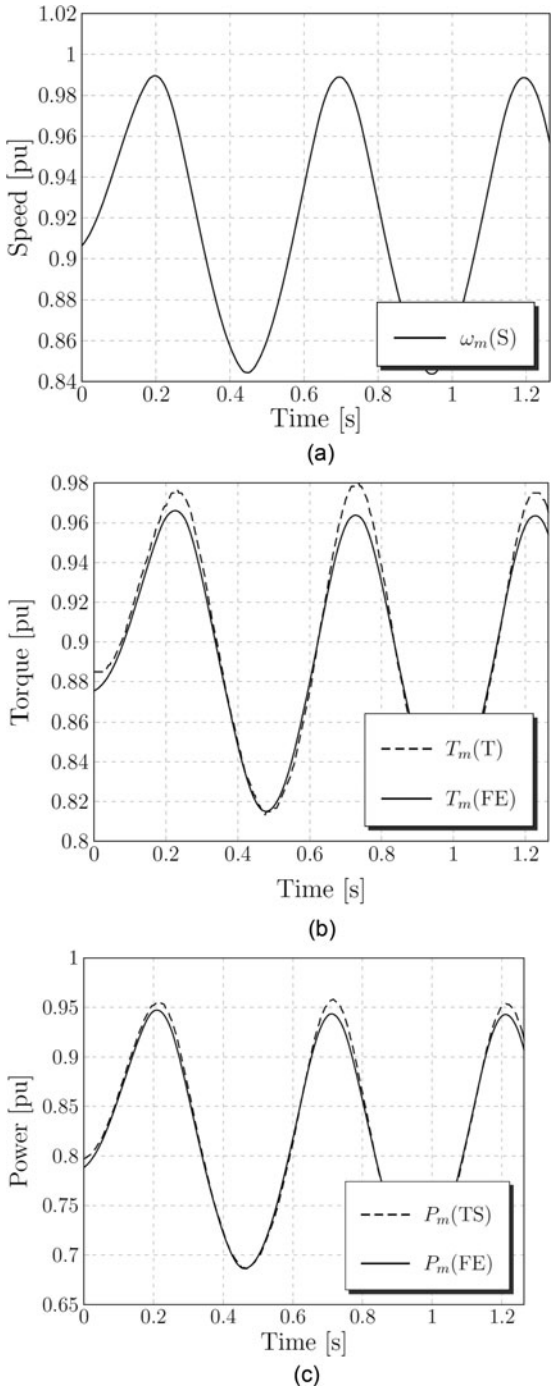

FIGURE 11. Measured dynamic test of the position sensorless controlled RSG drive.

a result of the digital low-pass filter in the control structure, implemented to smooth out the generator torque. The low-pass filter of the estimated speed, which is used in Eq. (12), also affects the MPPT. The dynamic performance, however, is still satisfactory.

6. CONCLUSION

A position sensorless controlled RSG with an LC inverter output filter for high-speed geared wind generators is proposed and evaluated. The proposed generator configuration allows the converter to be stationed in the turbine tower in-

stead of the nacelle. This configuration has weight advantages and possible converter maintenance advantages. It is shown that an estimation scheme is derived to estimate stator quantities to avoid the need for additional sensors on the machine side of the LC filter. The derived estimation method only uses the filter parameters to calculate the stator current and voltage.

Experimental evaluation shows that the LC filter ensures sinusoidal stator voltages. It is also shown that the derived estimation method is successful in estimating the stator quantities, hence eliminating the need for additional measuring sensors. A hybrid position sensorless control method is proposed to control the RSG. The hybrid method makes use of an HF injection position sensorless control method at standstill and low speeds and a fundamental saliency position sensorless control method from minimum to high speeds. The injection frequency of the HF injection position sensorless control method is chosen just below the resonance frequency of the filter to boost the HF current response. By carefully choosing the injection frequency, it was possible to halve the magnitude of the injection voltage. A novel implementation of the fundamental saliency position sensorless control method with the inverter LC filter revealed that position estimation is not possible with the inverter quantities. Using the estimated stator quantities does, however, stabilize the method. It is also found that the load-dependent compensation curve should be measured with the LC filter connected.

Laboratory tests show that it is possible to control the RSG position sensorless with an LC inverter output filter and the proposed stator quantity estimation method. Results show good correlation between the reference MPPT torque and the measured torque. Measured results shows good dynamic response of the RSG.

REFERENCES

[1] Potgieter, J. H. J., and Kamper, M. J., "Design of new concept direct grid-connected slip-synchronous permanent-magnet wind generator," *IEEE Trans. Ind. Appl.*, Vol. 48, No. 3, pp. 913–922, May/June 2012.

[2] Li, H., and Chen, Z., "Overview of different wind generator systems and their comparisons," *IET Renew. Power Generat.* Vol. 2, No. 2, pp. 123–138, 2008.

[3] Blaabjerg, F., and Ma, K., "Future on power electronics for wind turbine systems," *IEEE J. Emerging Selected Topics Power Electron.*, Vol. 1, No. 3, pp. 139–152, 2013.

[4] Blaabjerg, F., Chen, Z., Teodorescu, R., and Iov, F., "Power Electronics in wind turbine systems," *CES/IEEE 5th International Power Electronics and Motion Control Conference*, Vol. 1, pp. 1–11, 2006.

[5] Blaabjerg, F., Iov, F., Chen, Z., and Ma, K., "Power electronics and controls for wind turbine systems," *IEEE International Energy Conference and Exhibition (EnergyCon)*, pp. 333–344, Manama, Bahrain, 18–22 December 2010.

[6] Backlund, B., and Ebner, S., "The wind power converter for tomorrow is already here," *Technical Report, ABB Switzerland Ltd, Semiconductors*.

[7] ABB, "PCS 6000 for large wind turbines Medium voltage, full power converters up to 9 MVA," *ABB Technicla Report*.

[8] ABB, "ABB wind turbine converters Increased turbine output for creating the perfect wind economy," *ABB Technicla Report*.

[9] Busca, C., Stan, A.-I., Stanciu, T., and Stroe, D.-I., "Control of permanent magnet synchronous generator for large wind turbines," *IEEE International Symposium on Industrial Electronics (ISIE)*, pp. 3871–3876, Bari, Italy, 4–7 July 2010.

[10] Beng, G., *Sensorless Direct Torque and Flux Control of Interior Permanent Magnet Synchronous Motors at Very Low Speeds Including Standstill*, Ph. D. Dissertation, School of Electrical Engineering and Telecommunications, University of New South Wales, Sydney, Australia, 2010.

[11] Zhang, Z., Zhao, Y., Qiao, W., and Liyan, Q., "A space-vector modulated sensorless direct-torque control for direct-drive PMSG wind turbines," *IEEE Industry Applications Society Annual Meeting (IAS)*, pp. 1–7, Las Vegas, NV, 7–11 October 2012.

[12] Pontt, J., Rodriguez, J., Kouro, S., Silva, C., Farias, H., and Rotella, M., "Output sinus filter for medium voltage drive with direct torque control," *Conference Record of the 2005 40th IAS Annual Meeting. Industry Applications Conference*, Vol. 1, pp. 204–209, 2005.

[13] Steinke, J. K., "Use of an LC filter to achieve a motor-friendly performance of the PWM voltage source inverter," *IEEE Trans. Energy Conver.*, Vol. 14, No.3, pp. 649–654, 1999.

[14] Wu, B., Lang, Y., Zargari, N., and Kouro, S., *Power Conversion and Control of Wind Energy Systems, IEEE Press Series on Power Engineering*, Wiley-IEEE Press, Chap. 5, 2011.

[15] Bonnett, A. H., "Analysis of the impact of pulse-width modulated inverter voltage waveforms on AC induction motors," *IEEE Trans. Ind. App.* Vol. 32, No. 2, pp. 386–392, 1996.

[16] Von Jouanne, A., and Enjeti, P. N., "Design considerations for an inverter output filter to mitigate the effects of long motor leads in ASD applications," *IEEE Trans. Ind. Appl.*, Vol. 33, No. 5, pp. 1138–1145, 1997.

[17] Fukao, T., Yang, Z., and Matsui, M., "Voltage control of super high-speed reluctance generator system with a PWM voltage source converter," *IEEE Trans. Ind. Appl.*, Vol. 28, No. 4, pp. 880–886, 1992.

[18] Fukao, T., "Principles and output characteristics of super high-speed reluctance generator system," *IEEE Trans. Ind. Appl.*, Vol. IA-22, No. 4, pp. 702–707, 1986.

[19] Boldea, I., Fu, Z. X., and Nasar, S. A., "High-performance reluctance generator," *Elect. Power Appl., IEE Proc. B*, Vol. 140, No. 2, pp. 124–130, 1993.

[20] Boldea, I., Fu, Z., and Nasar, S. A., "Sensorless DC output control of a high performance reluctance generator system," *Conference Record of the 1994 IEEE Industry Applications Society Annual Meeting*, Vol. 1, pp. 16–22, 1994.

[21] Braun, M., Lehmann, O., and Roth-Stielow, J., "Sensorless rotor position estimation at standstill of high speed PMSM drive with LC inverter output filter," *2010 IEEE International Conference*

on, Industrial Technology (ICIT), pp. 410–415, Viña del Mar, Chile, 14–17 March 2010.

[22] Batzel, T. D., and Lee, K. Y., "Electric propulsion with sensorless permanent magnet synchronous motor: Implementation and performance," *IEEE Trans. Energy Convers.*, Vol. 20, No. 3, pp. 575–583, 2005.

[23] Piippo, A., Salomaki, J., and Luomi, J., "Signal injection in sensorless PMSM drives equipped with inverter output filter," *IEEE Trans. Ind. Appl.* Vol. 44, No. 5, pp. 1614–1620, 2008.

[24] Polinder, H., Ferreira, J. A., Jensen, B. B., Abrahamsen, A. B., Atallah, K., and McMahon, R. A., "Trends in wind turbine generator systems," *IEEE J. Emerging Selected Topics Power Electron.*, Vol. 1, No. 3, pp. 174–185, 2013.

[25] Germishuizen, J. J., Van der Merwe, F. S., Van der Westhuizen, K., and Kamper, M. J., "Performance comparison of reluctance synchronous and induction traction drives for electrical multiple units," *Conference Record of the 2000 IEEE Industry Applications Conference*, Vol. 1, pp. 316–323, 2000.

[26] Boglietti, A., Cavagnino, A., Pastorelli, M., and Vagati, A., "Experimental comparison of induction and synchronous reluctance motors performance," *Conference Record of the 2005 Fourtieth IAS Annual Meeting Industry Applications Conference*, Vol. 1, pp. 474–479, 2005.

[27] Fischer, K., Stalin, T., Ramberg, H., Thiringer, T., Wenske, J., and Karlsson, R., "Investigation of converter failure in wind turbines," Technical Report, Elforsk 2012.

[28] WinWinD, Technical Report, available at: http://www.winwind.com/the-new-winwind3.aspx.

[29] LORC Knowledge, "Alpha ventus offshore wind farm," Technical Report, available at: http://www.lorc.dk/offshore-wind-farms-map/alpha-ventus?lat=54.0202&lon=6.6062.

[30] Lettl, J., Bauer, J., and Linhart, L., "Comparison of different filter types for grid connected inverter," *Progress in Electromagnetics Research Symposium (PIERS)*, Marrakesh, Morocco, 20–23 March 2011.

[31] Salomaki, J., Piippo, A., Hinkkanen, M., and Luomi, J., "Sensorless vector control of PMSM drives equipped with inverter output filter," *32nd Annual Conference on IEEE Industrial Electronics (IECON 2006)*, pp. 1059–1064, Paris, France, 6–10 November 2006.

[32] Villet, W. T., Kamper, M. J., Landsmann, P., and Kennel, R., "Hybrid position sensorless vector control of a reluctance synchronous machine through the entire speed range," *15th International Power Electronics and Motion Control Conference (EPE/PEMC)*, Novi Sad, Serbia, 4–6 September 2012.

[33] Neammanee, B., Sirisumrannukul, S., and Chatratana, S., "Control strategies for variable-speed fixed-pitch wind turbines, wind power," in *Wind Power*, S. M. Muyeen (Ed.), Rijeka, Croatia: InTech, Chap. 9, 2010.

BIOGRAPHIES

Wikus T. Villet received the B.Eng. and Ph.D. in electric and electronic engineering in 2010 and 2014, respectively, from the University of Stellenbosch, South Africa. He is currently the lead systems design engineer at Powermote Drive Systems where he specializes in variable-speed drive and electrical motor control system design. His research is focused on position sensorless control methods of reluctance synchronous machines.

Maarten J. Kamper received the M.Sc. (Eng) and Ph.D. (Eng) from the Stellenbosch University, South Africa, in 1987 and 1996, respectively. In 1989, he joined the academic staff of the Department of Electrical and Electronic Engineering, Stellenbosch University, where he is currently a professor of electrical machines and drives. He is a South African National Research Foundation supported scientist and a registered professional engineer in South Africa. He is a senior member of the IEEE and acts as associate editor of the Electric Machine Committee of the *IEEE Transactions on Industry Applications*. He also serves on the steering committee of the International Conference on Electrical Machines (ICEM). His research areas are computer-aided design and the control of reluctance, permanent magnet, and induction electrical machine drives, with applications in electric transportation and renewable energy.